CR 137702
AVAILABLE TO PUBLIC

AN INVESTIGATION ON THE EFFECT OF SECOND-ORDER ADDITIONAL THICKNESS DISTRIBUTIONS TO THE UPPER SURFACE OF AN NACA 64-206 AIRFOIL

FEBRUARY 1975

CONTRACT NAS 2-8599

ANTONY W. MERZ

DONALD S. HAGUE

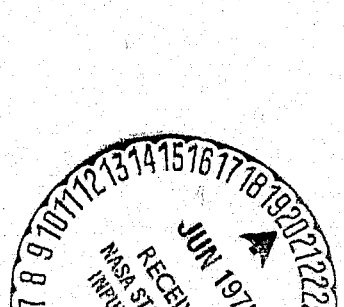

Prepared by

AEROPHYSICS RESEARCH CORPORATION

BELLEVUE, WASHINGTON 98009

Originally Published as

Aerophysics Research Corporation TN-195

TABLE OF CONTENTS

LIST OF ILLUSTRATIONS

ABSTRACT

This report describes a series of low speed airfoil designs based on modifications to the NACA 64-206 airfoil. Designs are based on potential flow theory. The report describes one of a series of airfoil modifications carried out under Contract NAS 2-8599, Application of Multivariable Search Techniques to Optimal Wing Design in Non-Linear Flow Fields. Mr. Raymond Hicks of National Aeronautics and Space Administration's Aeronautical Division, Ames Research Center, served as contract monitor for the present study.

AN INVESTIGATION ON THE EFFECT OF SECOND-ORDER ADDITIONAL THICKNESS DISTRIBUTIONS TO THE UPPER SURFACE OF AN NACA 64-206 AIRFOIL

by Antony W. Merz and Donald S. Hague

Aerophysics Research Corporation

SUMMARY

An investigation has been conducted on the Lawrence Radiation Center, Berkeley, CDC 7600 digital computer to determine the effects of additional thickness distributions to the upper surface of an NACA 64-206 airfoil. Additional thickness distributions employed were in the form of two second-order polynomial arcs which have a specified thickness, $\bar{y}$, at a given chordwise location, $\bar{x}$. The forward arc disappears at the airfoil leading edge, the aft arc disappears at the airfoil trailing edge. At the juncture of the two arcs, $x = \bar{x}$, continuity of slope is maintained. The effect of varying the maximum additional thickness and its chordwise location on airfoil lift coefficient, pitching moment, and pressure distribution was investigated. Results were obtained at a Mach number of 0.2 with an angle-of-attack of 6^{o} on the basic NACA 64-206 airfoil. All calculations employ the full potential flow equations for two dimensional flow. The relaxation method of Jameson is employed for solution of the potential flow equations.

Introducing this type of upper surface modification to the NACA 64-206 airfoil produced results which generally follow trends found previously in a similar investigation employing the NACA 64_1-212 airfoil. Increases in the rearward location of the maximum additional thickness and increases in the magnitude of the additional thickness both produce increases in the airfoil lift coefficient. Conversely moving the location of maximum thickness forward or decreasing the maximum thickness both reduce the magnitude of the quarter chord pitching moment. The magnitude of the largest pressure peak varies in a complicated manner with maximum additional

thickness and its chordwise location. For maximum thickness locations forward of the 2/3 chord additional thickness initially produces a reduction in pressure peak with a lift coefficient increase. With larger amounts of additional thickness pressure peak value and lift coefficient tend to rise together. This reversal in C_L-$C_{P_{max}}$ trend results from the creation of a second peak pressure region aft of the basic airfoil leading edge pressure peak. As thickness increases the magnitude of this aft peak rises while the magnitude of the leading edge pressure peak decreases. Minimum $C_{P_{max}}$ occurs when the two peak pressure values are equal. Further increases in thickness beyond this point produce simultaneous increases in both lift coefficient and peak pressure. Solutions were difficult to obtain for the thicker airfoils during the present study. Increased lift, and its accompanying circulation around the relatively sharp leading edge of the NACA airfoil, caused numerical difficulties in solution of the potential flow equation for these equations. This effect was most pronounced for aft location of maximum additional thickness.

For maximum thickness locations aft of the 2/3 chord location additional thickness produces a monotonic rise in both lift coefficient and pressure peak magnitude. In these cases the leading edge pressure peak always dominates. A consequence of the above behavior is that for a given lift coefficient value the peak pressure can be minimized by careful selection of the location of maximum thickness and its magnitude. Generally as the lift coefficient rises the maximum thickness location moves aft. For lift coefficients between 1.0 and 1.6, the chordwise location of the maximum thickness varied from 10% to 30%. For this increase in lift coefficient, the magnitude of the peak pressure coefficient decreases from about 3 to 2.4.

It should be noted that viscous effects are neglected in the present analysis. At the higher lift coefficients the effect of viscosity could be significant. Further investigations incorporating a viscous flow model are therefore desirable.

INTRODUCTION

The National Aeronautics and Space Administration and others are currently conducting a series of theoretical and experimental studies to define airfoil sections having improved performance from the aspects of lift, drag, pitching moment or pressure distribution characteristics, references 1 and 2. Analytic investigations using airfoil surface representations based on high-order polynomials may result in impractical profiles, for example, very thin trailing edge thickness distributions or severe reflexes in the profile. The present study employs low-order polynomial arcs of second-order whose characteristics are selected to avoid such problems. Previous optimization studies using multivariable search techniques, references 1, 3 and 4, generally indicate that shape changes which provide increased lift produce unfavorable changes in moment characteristics. Conversely profile changes which improve the moment characteristics decrease the lift coefficient. With the low-order model of the present investigation a systematic examination on the effect of profile changes can be carried out. This was accomplished and the trends previously revealed by optimization studies were confirmed. An interesting by product of the systematic investigation of profile changes and that of the previous investigation of the NACA 64_1-212 airfoil is that a gain in lift coefficient can be produced while reducing the peak negative pressures. This tends to decrease the pressure gradient and hence holds promise for the development of practical single component high lift coefficient airfoils.

MATHEMATICAL MODELS

Potential Flow Equation

Potential flow analysis is based on solution of the two-dimensional potential flow equation

$$(a^2-u^2)\,\phi_{xx} + (a^2-v^2)\,\phi_{yy} - 2uv\,\phi_{xy} = 0$$

where ϕ is the velocity potential, u and v are the velocity components

$$u = \phi_x, \quad v = \phi_y$$

and a is the local speed of sound determined from the energy equation and the stagnation speed of sound

$$a^2 = a_o^2 - \left(\frac{\gamma - 1}{2}\right) \quad (u^2 + v^2)$$

Solutions are obtained by Jameson's finite difference scheme, reference 5.

AIRFOIL PROFILE REPRESENTATION

Basic Airfoil

Ordinates for the basic NACA 64-206 airfoil were approximated by four cubic chain polynomials in the manner of Hicks

$$y_j = a_{o_j} F_1 + a_{1_j} x + a_{2_j} x^2 + a_{3_j} x^3; \quad j = 1,2,3,4$$

Coefficients in the four polynomial arcs are selected on the following basis:

i = 1 - Arc represents forward portion of upper surface

$$F_1 = \sqrt{x}$$

i = 2 - Arc represents aft portion of upper surface

$$F_2 = 1$$

i = 3 - Arc represents forward portion of lower surface

$$F_3 = \sqrt{x}$$

i = 4 - Arc represents aft portion of lower surface

$$F_4 = 1$$

The coefficients a_{i_j} are determined by introducing four boundary conditions on the airfoil profile in each of the four airfoil arcs. Crout's method for triangularization and back substitution is used to solve the resulting system of linear equations. Note that if four points are specified on the aft portion (i = 2 or 4), a discontinuity in slope occurs where the polynomials join. This produces a small ripple in the pressure distribution

at the juncture point. However, since the juncture occurs at a region of small slope (x = .5) the effect is not significant. The approximate NACA 64-206 airfoil developed by this method is presented in Figure 1.

Additional Thickness

In the present study additional thickness is limited to the upper airfoil surface. The additional thickness has the form

$$\Delta y(x) = \bar{y}\left[1 - \left(\frac{\bar{x}-x}{x}\right)^2\right]; \quad x < \bar{x}$$

$$\Delta y(x) = \bar{y}\left[1 - \left(\frac{\bar{x}-x}{1-\bar{x}}\right)^2\right]; \quad x \geq \bar{x}$$

These functions are of second-order varying parabolically with $\zeta = |x - \bar{x}|$. Additional thickness is zero at the leading edge (x = 0) and trailing edge (x = 1) and has a maximum of $\Delta y = \bar{y}$ at $x = \bar{x}$. Additional thickness and slope of the additional thickness are continuous throughout the interval $0 \leq x \leq 1$. The second derivative of the additional thickness distribution is constant in the forward and aft airfoil arcs but has a discontinuity at the arc junction, $x = \bar{x}$. It follows that a continuous polynomial representation of the additional thickness distributions, valid in the interval $0 \leq x \leq 1$ would be in the form of an infinite series. This type of additional thickness distribution is referred to as a "biquadratic" function in recognition of the above characteristics. A sequence of biquadratic arcs having varying maximum thickness positions is presented in Figure 2.

PREVIOUS OPTIMIZATION STUDIES

Lift Coefficient Maximization

Maximization of lift coefficient has the form

$$\emptyset = \text{Max}\left[C_L\right]$$

where

$$C_L = \oint \Delta p(x)\,dx$$

and the integration is around the airfoil contour. Since the airfoil

contour is completely described in terms of the two parameters $\bar{x}$ and $\bar{y}$

$$\phi = \text{Max}\left[C_L\right] = \text{Max}\left[C_L(\bar{x},\bar{y})\right]$$

where

$$\bar{x}_L \leq \bar{x} \leq \bar{x}_H$$

$$\bar{y}_L \leq \bar{y} \leq \bar{y}_H$$

This two variable multivariable search problem can be solved by a combination of directed random-ray and pattern searches, reference 3. Table I presents the results of 30 iterations previously obtained in the reference 4 study of the NACA 64_1-212 airfoil using these search procedures. Lift gains were produced at 27 of the 30 iterations and continued to be made at the computation termination.

Optimization moved the position of maximum thickness to the most rearward position allowed, $\bar{x} = 0.9$. At termination, lift was increasing monotonically with increasing thickness, $\bar{y}$. Based on this isolated result lift may be maximized for additional thickness of the form assumed by moving the position of maximum additional thickness as far aft as allowed and introducing as much additional thickness as allowed.

Moment Minimization

Minimization of the moment coefficient has the form

$$\phi = \text{Min}\left[C_M\right]$$

where

$$C_M = \oint (x - 1/4)\ \Delta p(x)dx$$

In previous studies moment minimization resulted in a solution directly opposed to lift maximization. The position of maximum thickness moved forward and the amount of additional thickness was minimized. Thus the basic airfoil tends to have less adverse moment than any airfoil generated by addition of biquadratic thickness to the upper surface of the airfoil.

Optimization Summary

Optimal airfoil results previously obtained in the reference 4 study are summarized in Table II. It can be seen that in all cases previously

studied the position of maximum thickness, $\bar{x}$, is either at the extreme forward or rearward position allowed. Similarly, depending on problem specification, the amount of additional thickness should be either minimized or maximized. The low dimensionality of this problem (two parameters, $\bar{x}$ and $\bar{y}$) permit a ready mapping of results obtained on the present modifications to a NACA 64-206 airfoil as a function of $\bar{x}$ and $\bar{y}$. This is done in the following section.

SYSTEMATIC VARIATION OF NACA 64-206 AIRFOIL SHAPING PARAMETERS

The present study of a NACA 64-206 airfoil was based on a systematic investigation on the effect of variations in the airfoil shaping parameters $\bar{x}$ and $\bar{y}$. The resulting airfoils and calculated pressure distributions are presented in Figures 3(a) to 3(v). The pressure signatures vary in a radical manner with $\bar{x}$ and $\bar{y}$. The basic airfoil exhibits a sharp pressure peak at the leading edge. Magnitude of the peak pressure is reduced by introducing additional thickness in a forward location, $\bar{x}$ = .1, and the leading edge pressure peak position moves aft. However, if the amount of additional thickness is further increased the pressure peak magnitude again increases. This peak is located well aft of the leading edge pressure peak. This result is due to the creation of a second peak in the upper surface pressure distribution. This effect persists until rearward locations of $\bar{x}$ are encountered. For example, (Figure 3(u)), introducing additional thickness at $\bar{x}$ = .7 theoretically results in a rearward "hump" in the pressure distribution somewhat similar to that produced by a trailing edge flap. At this extreme aft location the increased circulation produced by this pressure hump also produces an increased leading edge peak in the airfoil pressure distribution. Flow separation would probably be encountered with these rearward additional thickness distributions unless devices such as rotating cylinders or blowing were employed.

Figure 4 illustrates the effect of varying position of maximum thickness and maximum thickness on lift coefficient. It can be seen that lift coefficient is maximized by increasing both $\bar{x}$ and $\bar{y}$. Generally

Figure 4 confirms trends of optimization studies using the NACA 64_1-212 airfoil discussed in the previous section. The principal effect of changing reference airfoils from the NACA 64_1-212 to the NACA 64-206 is a reduction in the magnitude of pressure coefficients. The dashed lines of Figure 4 show the lift coefficient variation of the thicker NACA 64_1-212 airfoil (reference 4) superimposed on the results obtained with the NACA 64-206 airfoil. Lift coefficient values are displaced downward by a nearly constant amount when the NACA 64-206 airfoil is employed. Since the additional thickness and the basic 6% airfoil thickness are additive, Figure 4 presents lift coefficient as a function of thickness. To first-order the airfoil thickness required is

$$t/c = 6\% + \bar{y}$$

As $\bar{x}$ moves to the extremes of the range the actual airfoil thickness is less than this amount as the positions of maximum thickness on the basic and additional thickness distributions are significantly different.

Moment coefficient variation with $\bar{x}$ and $\bar{y}$ is presented in Figure 5. It can be seen that the increased lift available from additional thickness is accompanied by a matching increase in undesirable pitching moment coefficient. The conclusion of the previous section that moment coefficient is minimized by moving $\bar{x}$ forward and diminishing $\bar{y}$ is borne out by Figure 5, again confirming previous optimization study results in reference 4.

As has been noted above, the primary effect of reducing basic airfoil thickness from 12% to 6% is to reduce both the lift and the pitching moment coefficients. Figure 5 illustrates this effect for pitching moment coefficient. The solid line presents results obtained on the NACA 64-206 airfoil. The dashed lines superimpose previous results obtained with the NACA 64_1-212 airfoil.

Figure 6 provides another means of studying the simultaneous variations of C_L and C_M. That is, the desirable characteristics of high lift and low moment are attainable only in a relative or weighted sense (reference 4). For the NACA 64-206 airfoil, the C_L-C_M variation at a constant value of $\bar{x}$ is only nearly linear. The desired slope of this line is as small as possible. As shown in Figure 6, this is attained by making the point of maximum additional thickness close to the leading edge. The numeral

procedure, however, may not converge when the additional thickness is added too close to the leading edge. The dashed line of Figure 6 corresponds to $\bar{x} = .2$, and the data extend below this line for $\bar{x} = .1$ only at $\bar{y} = .03$ and .06 due to these numerical difficulties. However, the trend is clear when the C_M-C_L trade-off is measured by the line function criteria of reference 4. Maximum thickness should be employed and introduced as near to the leading edge as possible.

Figure 7 presents the relationship between pressure peak and lift coefficient fc · a range of $\bar{x}$ and $\bar{y}$ values. For each value of $\bar{y}$ (maximum additional thickness) there is a point at which the pressure peak magnitude is minimized. Cross plotting the peak pressures as a function of C_L in Figure 8 reveals the minimum peak pressures as a function of C_L.

Figure 9 plots the position of maximum additional thickness as a function of C_L. As C_L increases, $\bar{x}$ moves aft. The associated values of $\bar{y}$ required for the low peak pressure is also plotted in Figure 9. The amount of additional thickness required for a minimum pressure peak increases with C_L. Finally, Figure 10 plots the minimum C_p attainable as a function of C_L using the biquadratic additional thickness airfoil model. For the range of thicknesses studied here, $C_{p_{max}}$ reduces with C_L flattening out at $C_L = 1.5$. Minimum C_p values are higher than those attained in the Reference 4 study using the 64_1-212 airfoil.

CONCLUSION

A numerical investigation into a class of modified airfoil shapes has been completed using full two-dimensional flow potential flow equations. Airfoils studied were obtained by modifying the NACA 64-206 airfoil by additional thickness distributions based on a biquadratic variation with chordwise position. Free stream Mach number was held constant at $M = 0.2$ and the basic airfoil is held at 6^o angle-of-attack. Results of the study may be summarized as follows and are generally in agreement with reference 4:

1. Significant changes in pressure distribution, lift and pitching moment can be introduced by the biquadratic thickness modification.

2. The requirements for improving lift and moment coefficient characteristics are directly opposed to each other. That is, increases in lift result in increases in adverse moment. Conversely, decreases in adverse moment produce decreases in lift.

3. High lift airfoils require the addition of a thickness distribution biased to the rear of the foil and as much thickness addition as possible.

4. Low adverse moments require a thickness distribution biased to the front of the foil and as little additional thickness as possible. Therefore, the best airfoil based on moment considerations is the unmodified foil.

5. Favorable lift/moment trade-off characteristics are obtained by a thickness distribution biased to the front of the foil employing as much thickness as possible.

6. There exists a class of airfoil exhibiting low peak pressures for a given C_L which require an intermediate location of maximum additional thickness and thickness amount. Generally, the position of maximum additional thickness moves to the rear with increasing C_L, and the amount of additional thickness required increases with increasing C_L.

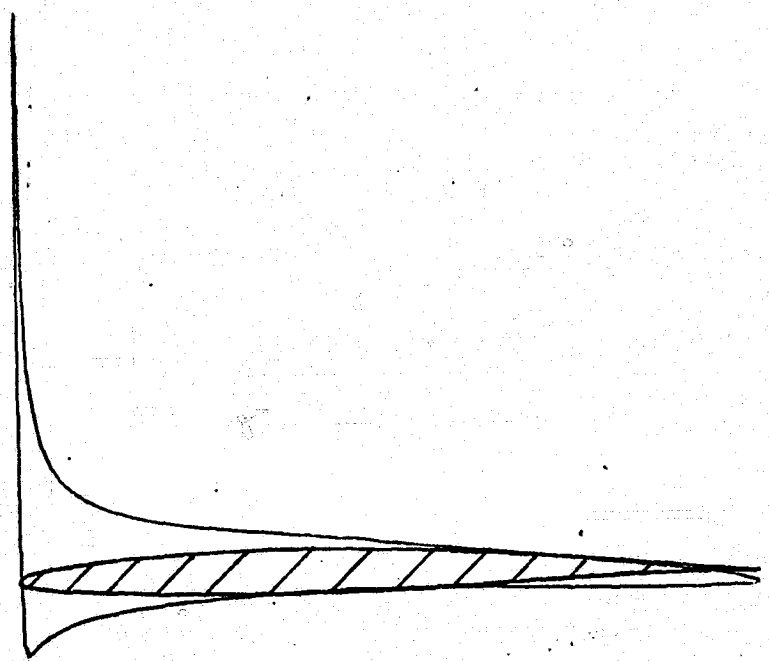

FIGURE 1. 64-206 AIRFOIL AND PRESSURE DISTRIBUTION

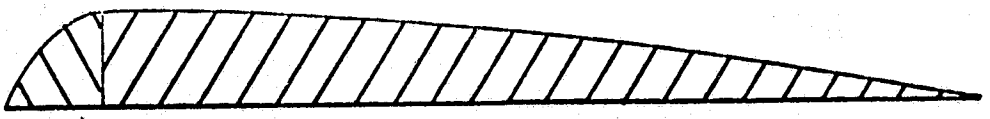

a) $\bar{x} = .1$

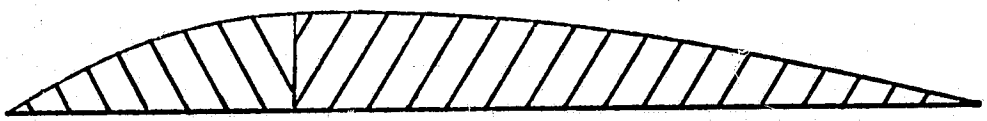

b) $\bar{x} = .3$

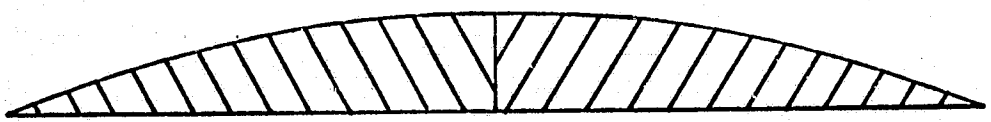

c) $\bar{x} = .5$

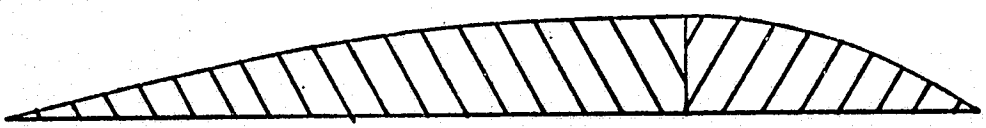

d) $\bar{x} = .7$

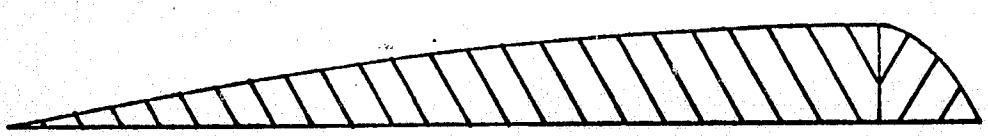

e) $\bar{x} = .9$

FIGURE 2 BIQUADRATIC ADDITIONAL THICKNESS DISTRIBUTIONS

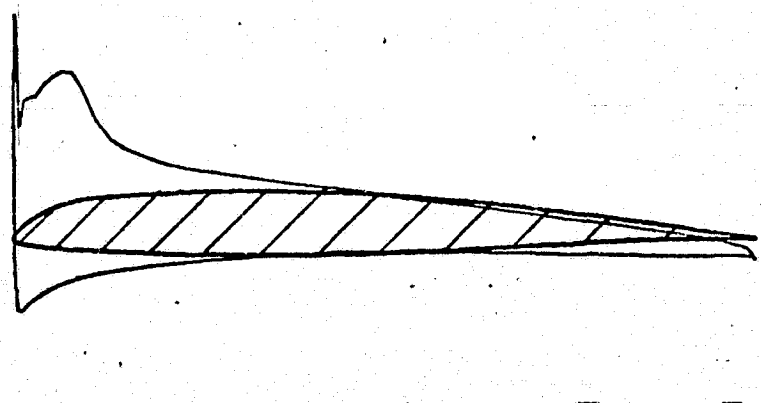

FIGURE 3(a). MODIFIED 64-206 AIRFOIL, $\bar{x} = .1$, $\bar{y} = .03$

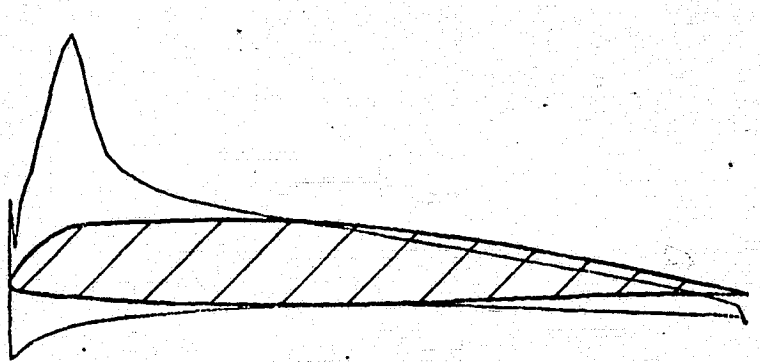

FIGURE 3(b). MODIFIED 64-206 AIRFOIL, $\bar{x} = .1$, $\bar{y} = .06$

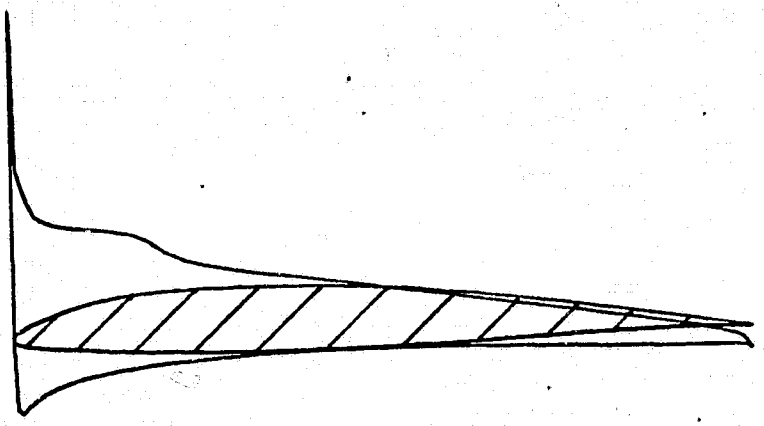

FIGURE 3(c). MODIFIED 64-206 AIRFOIL, $\bar{x}$ = .2, $\bar{y}$ = .03

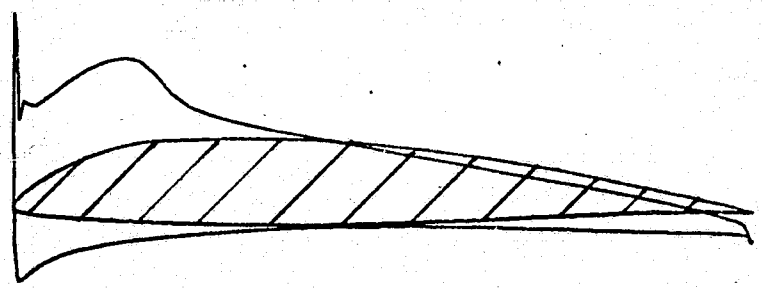

FIGURE 3(d). MODIFIED 64-206 AIRFOIL, $\bar{x}$ = .2, $\bar{y}$ = .06

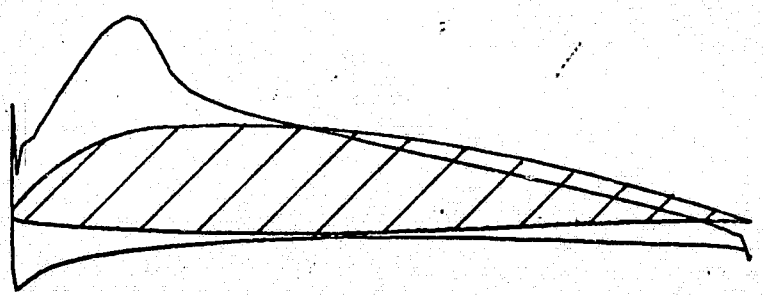

FIGURE 3(e). MODIFIED 64-206 AIRFOIL, $\bar{x}$ = .2, $\bar{y}$ = .09

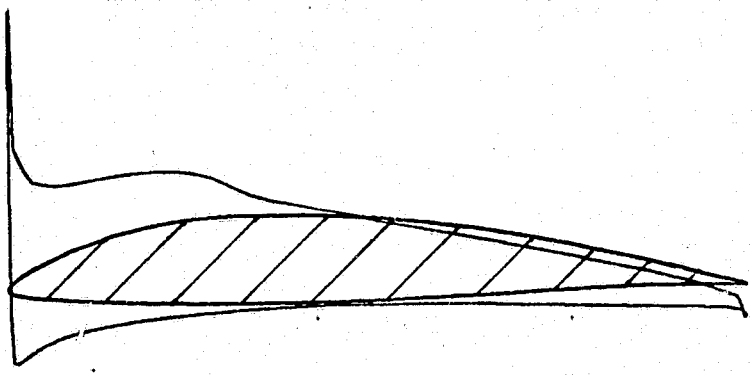

FIGURE 3(f). MODIFIED 64-206 AIRFOIL, $\bar{x}$ = .3, $\bar{y}$ = .06

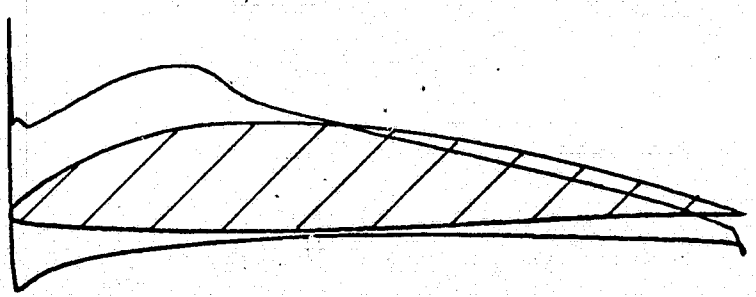

FIGURE 3(g). MODIFIED 64-206 AIRFOIL, $\bar{x}$ = .3, $\bar{y}$ = .09

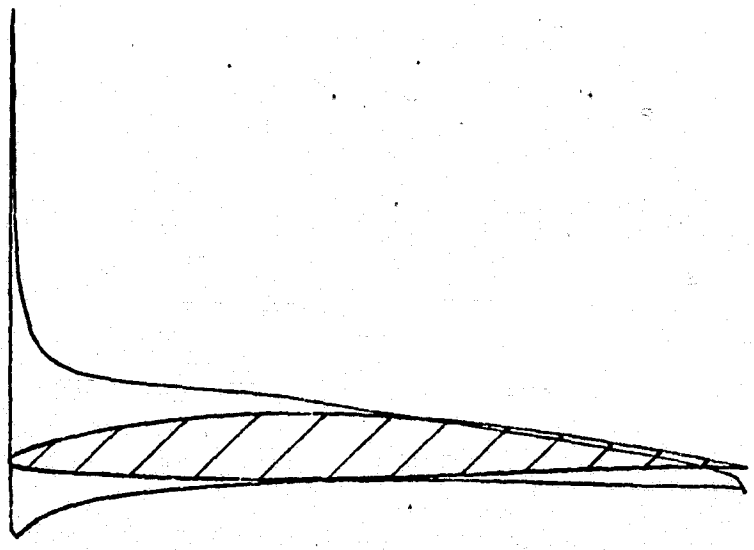

FIGURE 3(h). MODIFIED 64-206 AIRFOIL, $\bar{x}$ = .4, $\bar{y}$ = .03

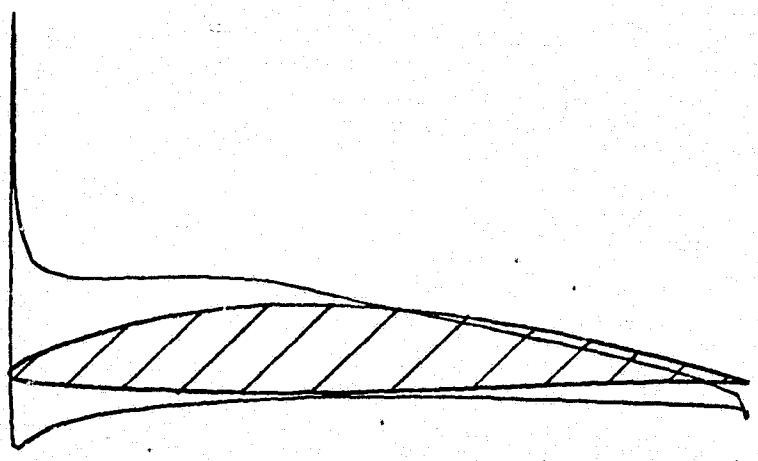

FIGURE 3(i). MODIFIED 64-206 AIRFOIL, $\bar{x}$ = .4, $\bar{y}$ = .06

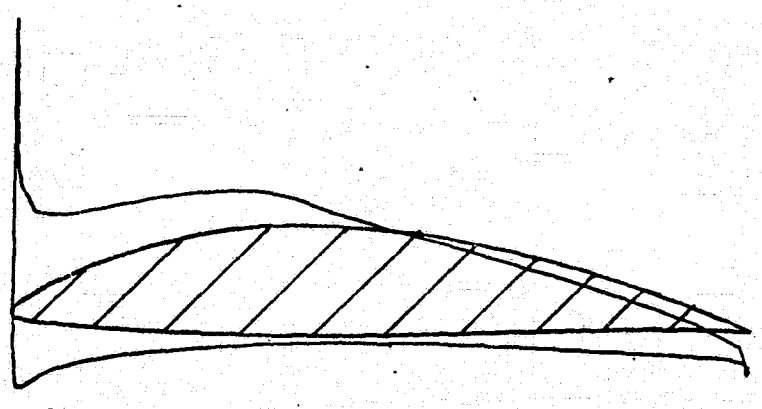

FIGURE 3(j). MODIFIED 64-206 AIRFOIL, $\bar{x}$ = .4, $\bar{y}$ = .09

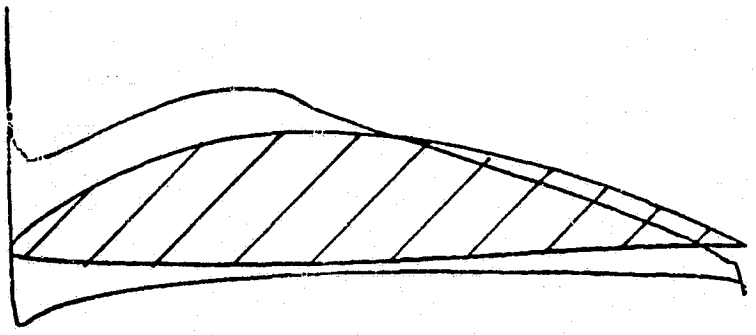

FIGURE 3(k). MODIFIED 64-206 AIRFOIL, $\bar{x} = .4$, $\bar{y} = .12$

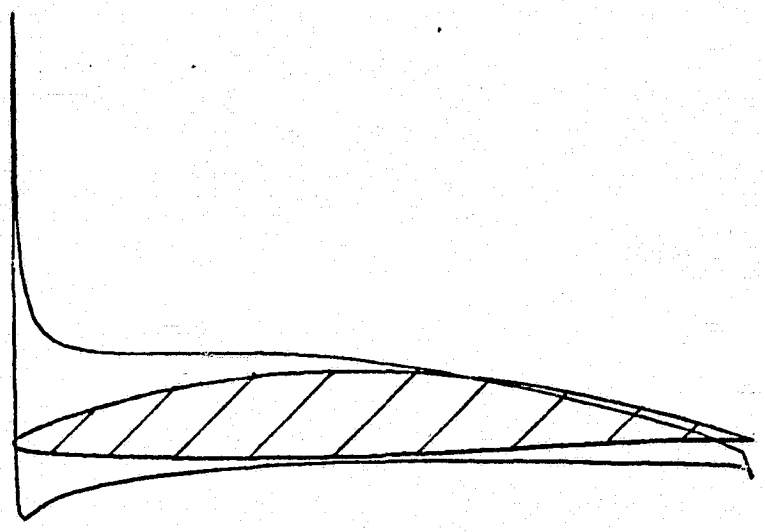

FIGURE 3(l). MODIFIED 64-206 AIRFOIL, $\bar{x} = .5$, $\bar{y} = .06$

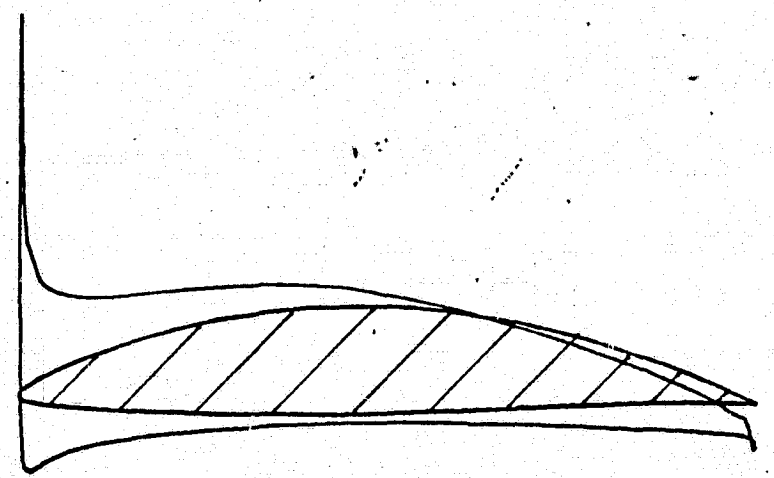

FIGURE 3(m). MODIFIED 64-206 AIRFOIL, $\bar{x} = .5$, $\bar{y} = .09$

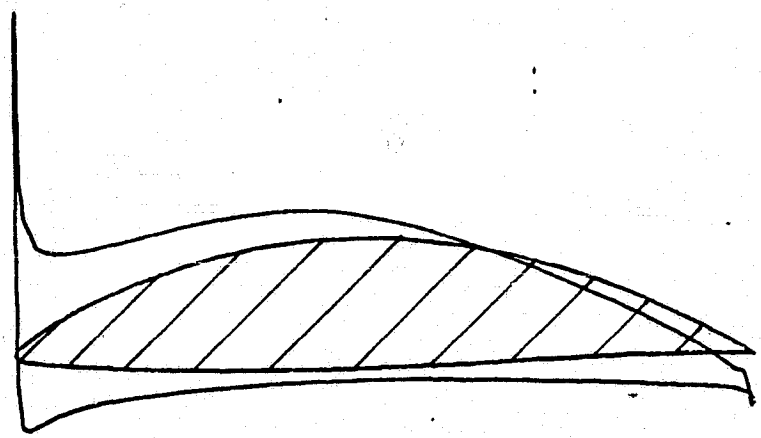

FIGURE 3(n). MODIFIED 64-206 AIRFOIL, $\bar{x}$ = .5, $\bar{y}$ = .12

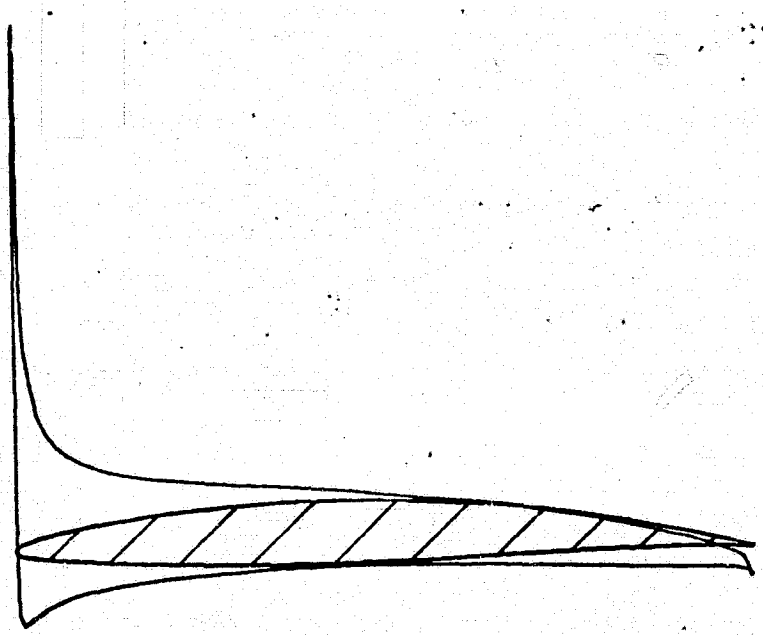

FIGURE 3(o). MODIFIED 64-206 AIRFOIL, $\bar{x}$ = .6, $\bar{y}$ = .03

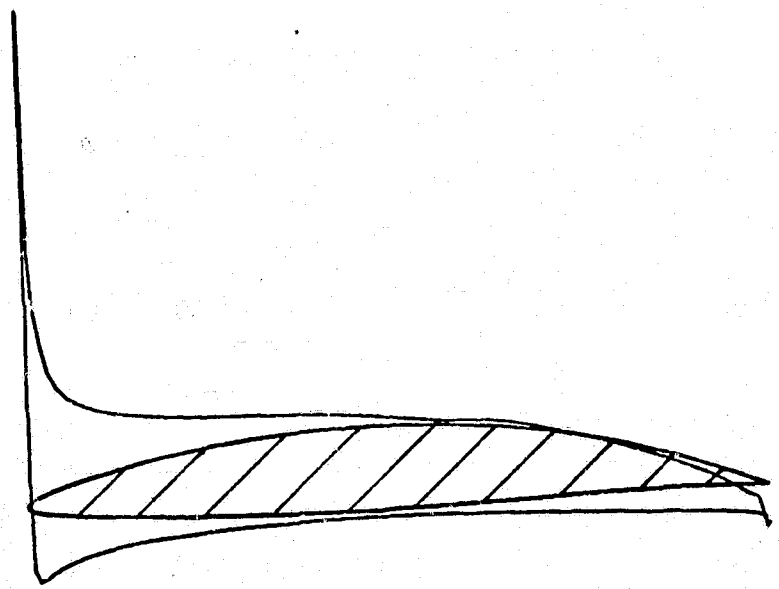

FIGURE 3(p). MODIFIED 64-206 AIRFOIL, $\bar{x} = .6$, $\bar{y} = .06$

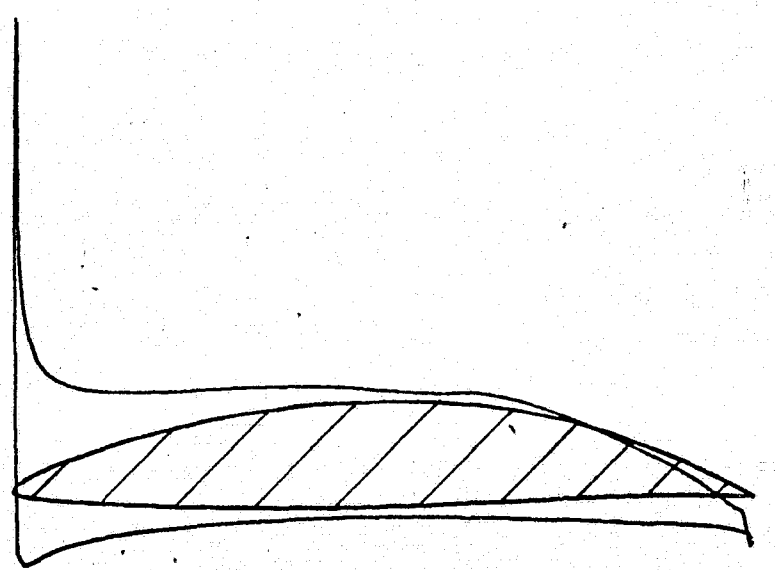

FIGURE 3(q). MODIFIED 64-206 AIRFOIL, $\bar{x} = .6$, $\bar{y} = .09$

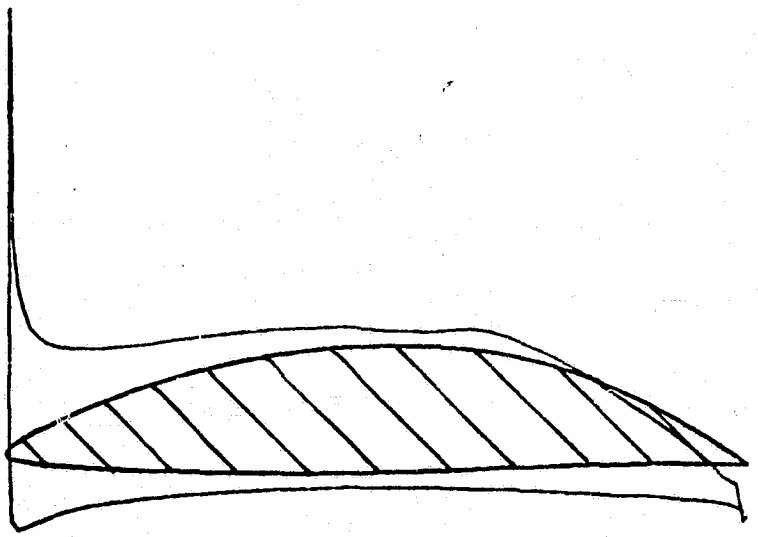

FIGURE 3(r). MODIFIED 64-206 AIRFOIL, $\bar{x}$ = .6, $\bar{y}$ = .12

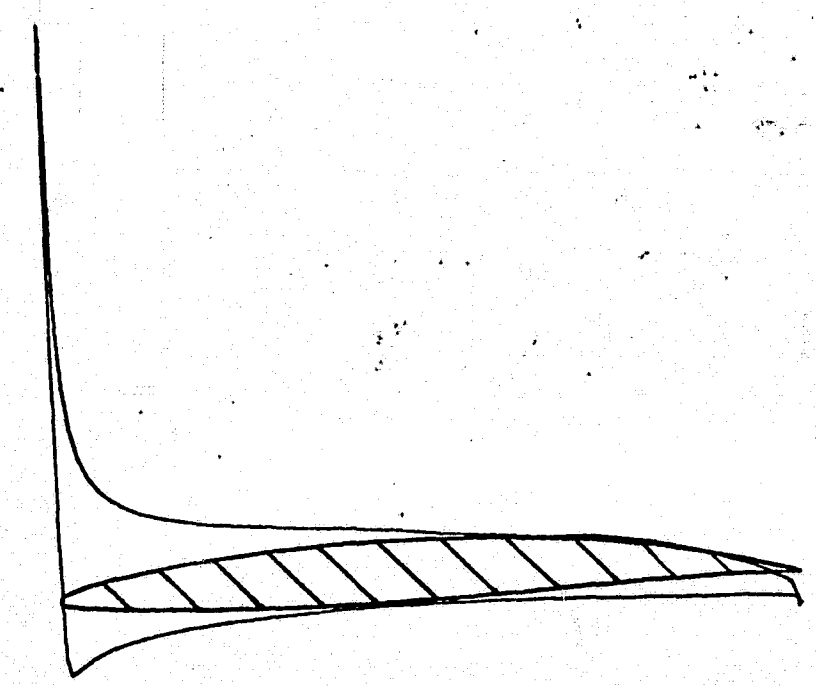

FIGURE 3(s). MODIFIED 64-206 AIRFOIL, $\bar{x}$ = .7, $\bar{y}$ = .03

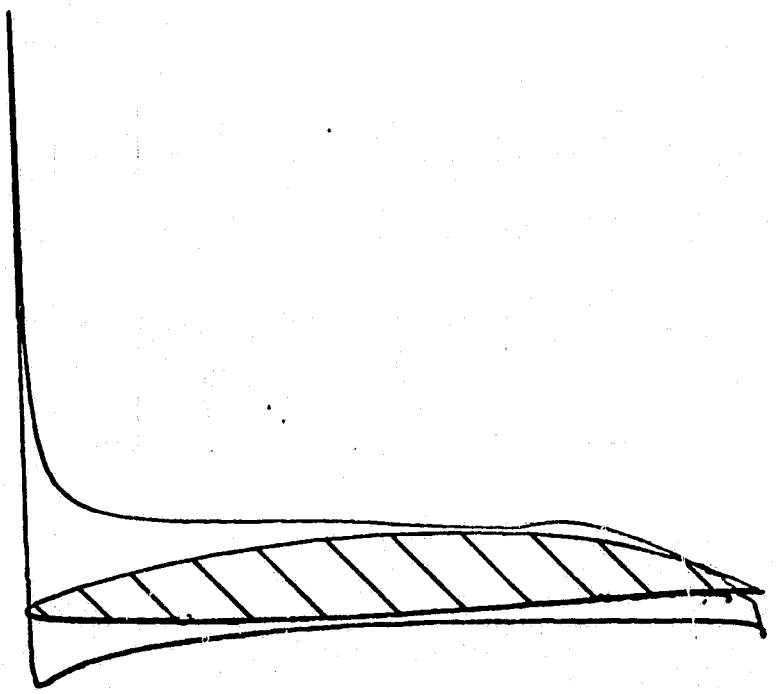

FIGURE 3(t). MODIFIED 64-206 AIRFOIL, $\bar{x}$ = .7, $\bar{y}$ = .06

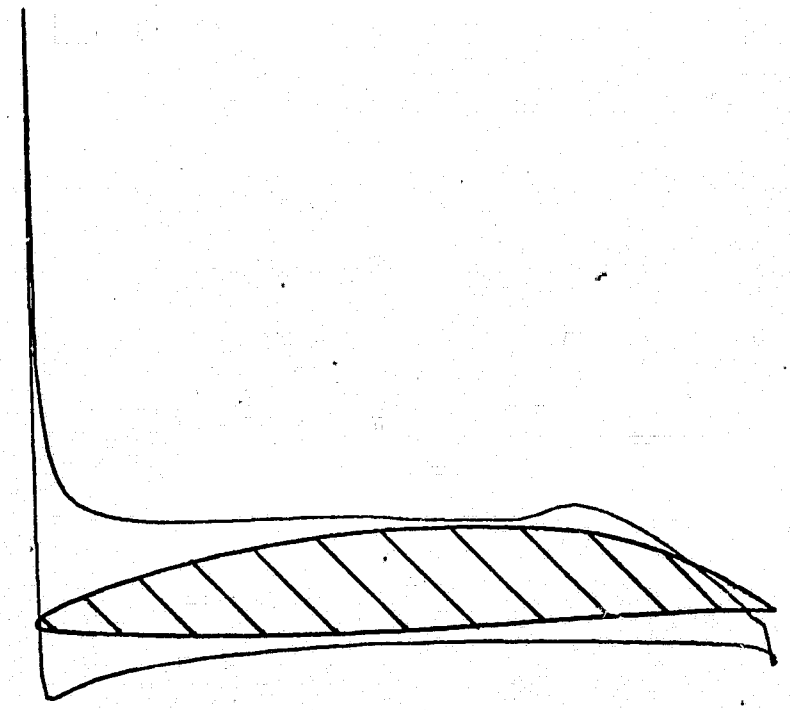

FIGURE 3(u). MODIFIED 64-206 AIRFOIL, $\bar{x}$ = .7, $\bar{y}$ = .09

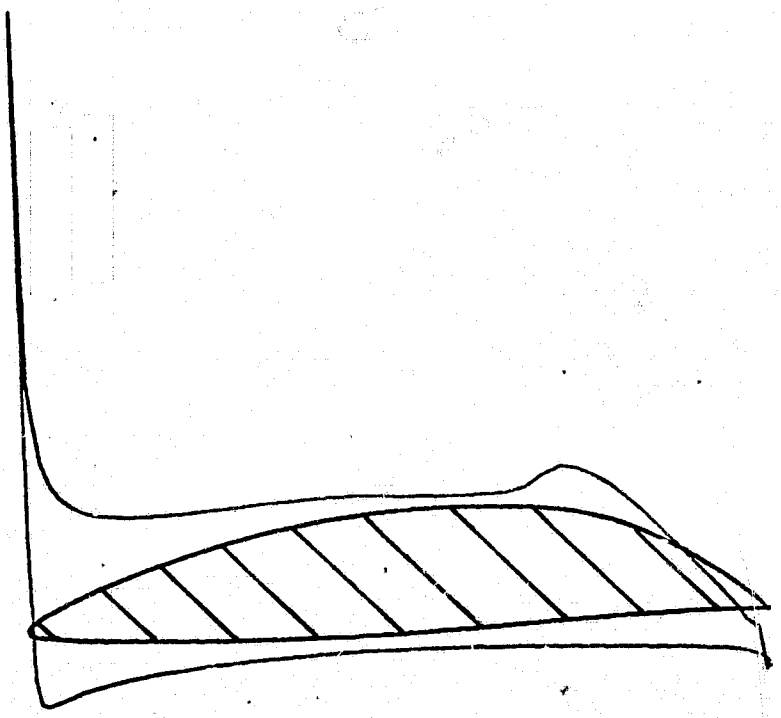

FIGURE 3(v). MODIFIED 64-206 AIRFOIL, $\bar{x} = .7$, $\bar{y} = .12$

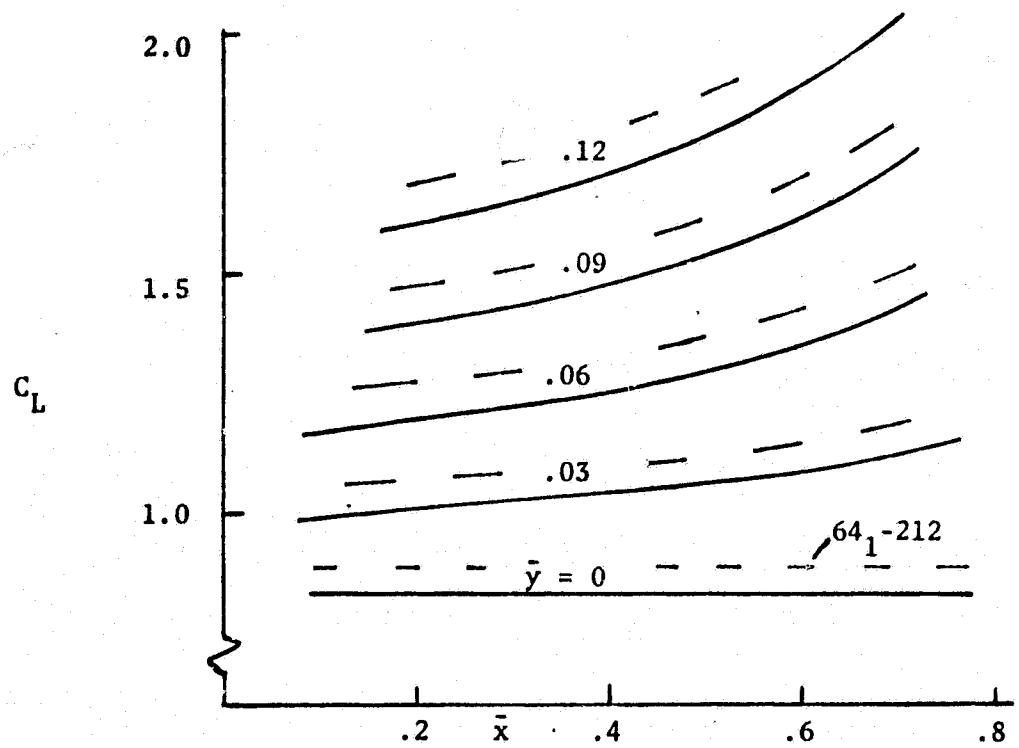

FIGURE 4. LIFT COEFFICIENT, BIQUADRATIC MODIFICATIONS TO 64-206

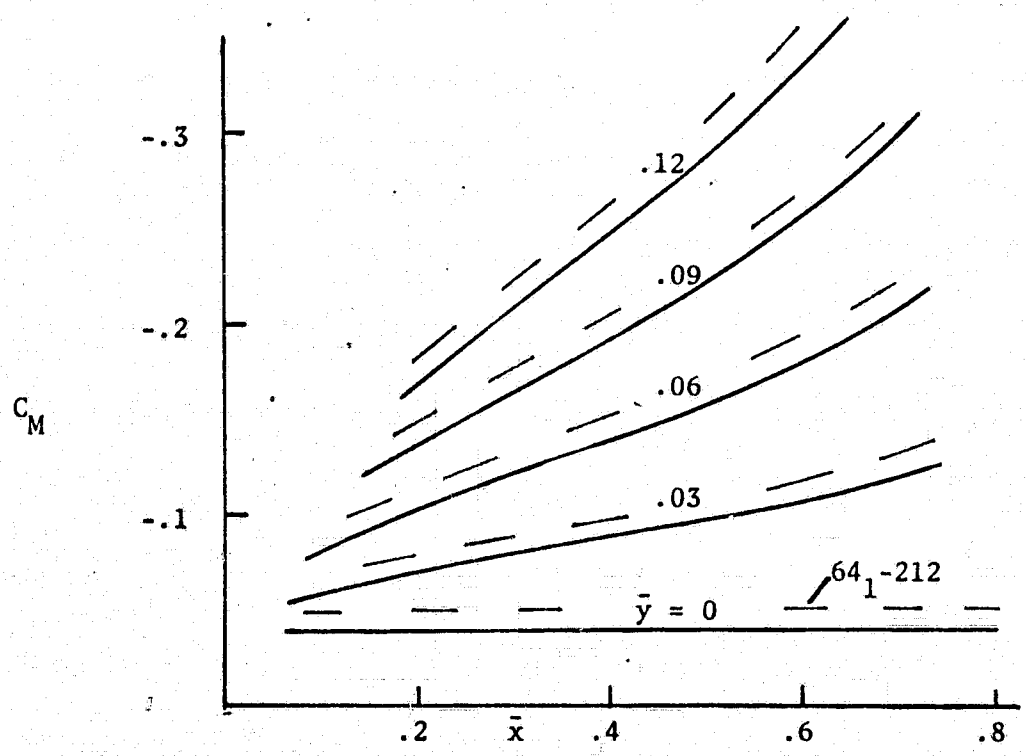

FIGURE 5. MOMENT COEFFICIENT, BIQUADRATIC MODIFICATIONS TO 64-206

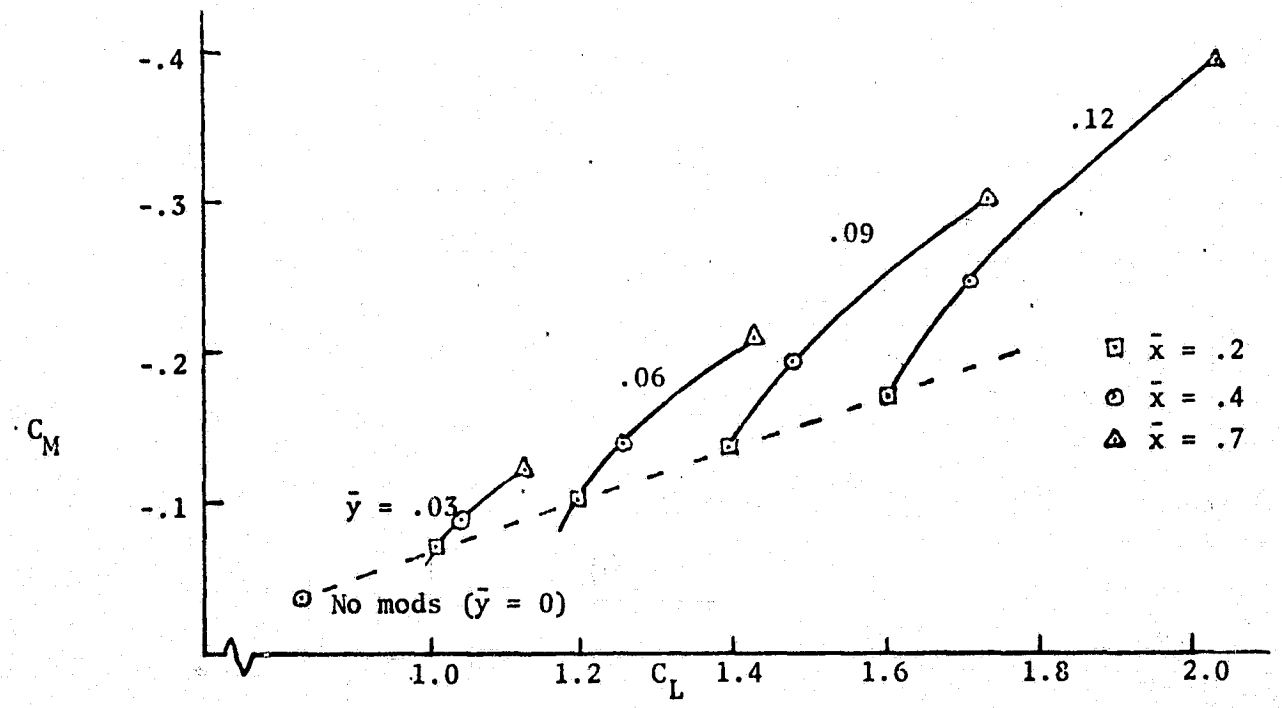

FIGURE 6. LIFT AND MOMENT VARIATIONS

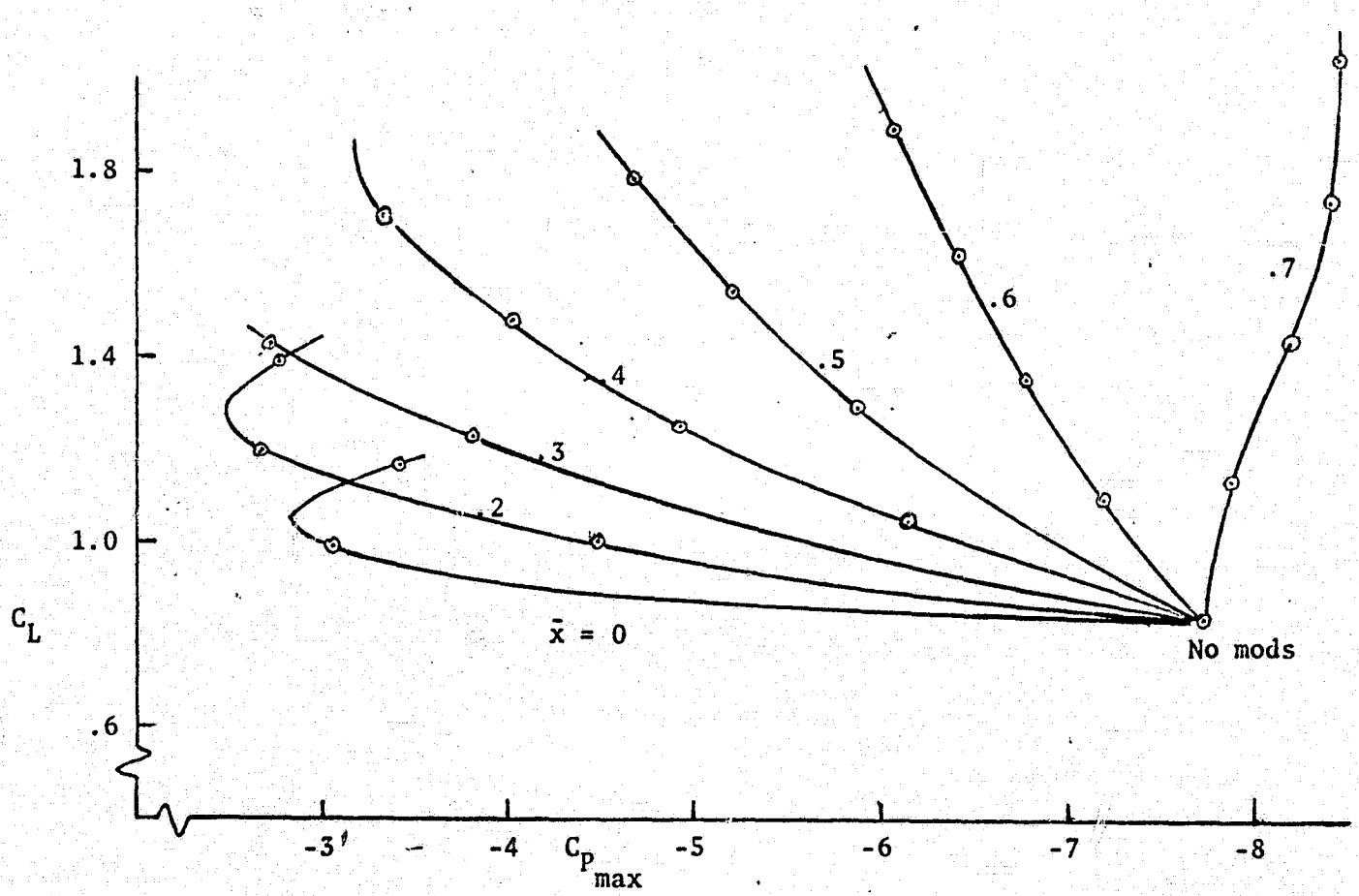

FIGURE 7. BIQUADRATIC MODIFICATIONS TO 64-206

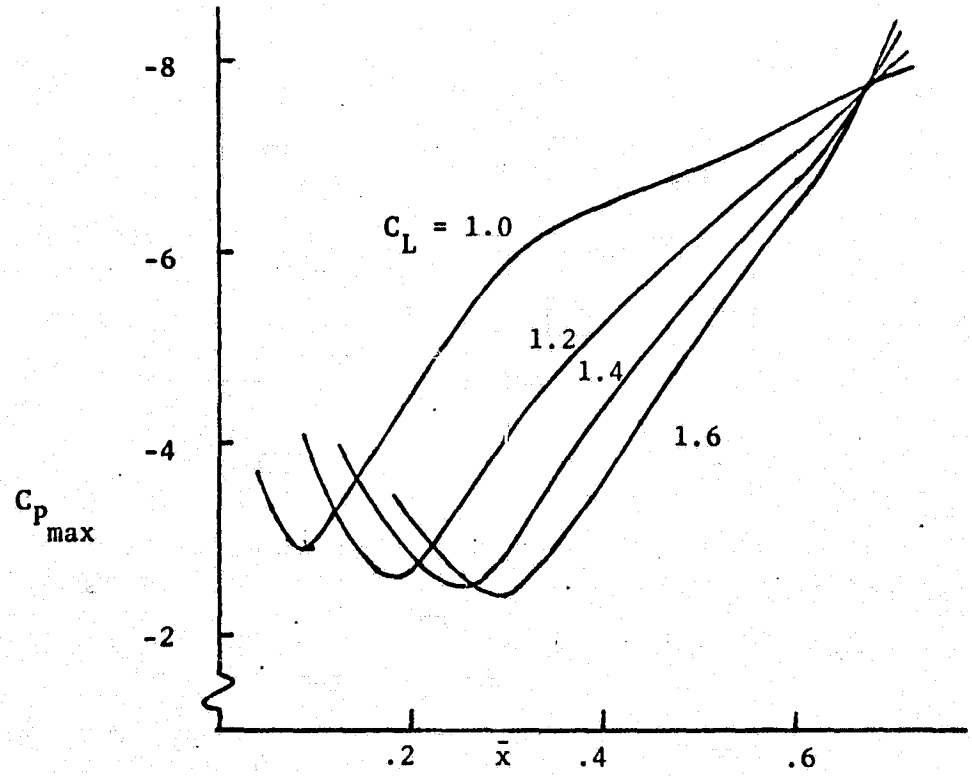

FIGURE 8. BIQUADRATIC MODIFICATIONS TO 64-206

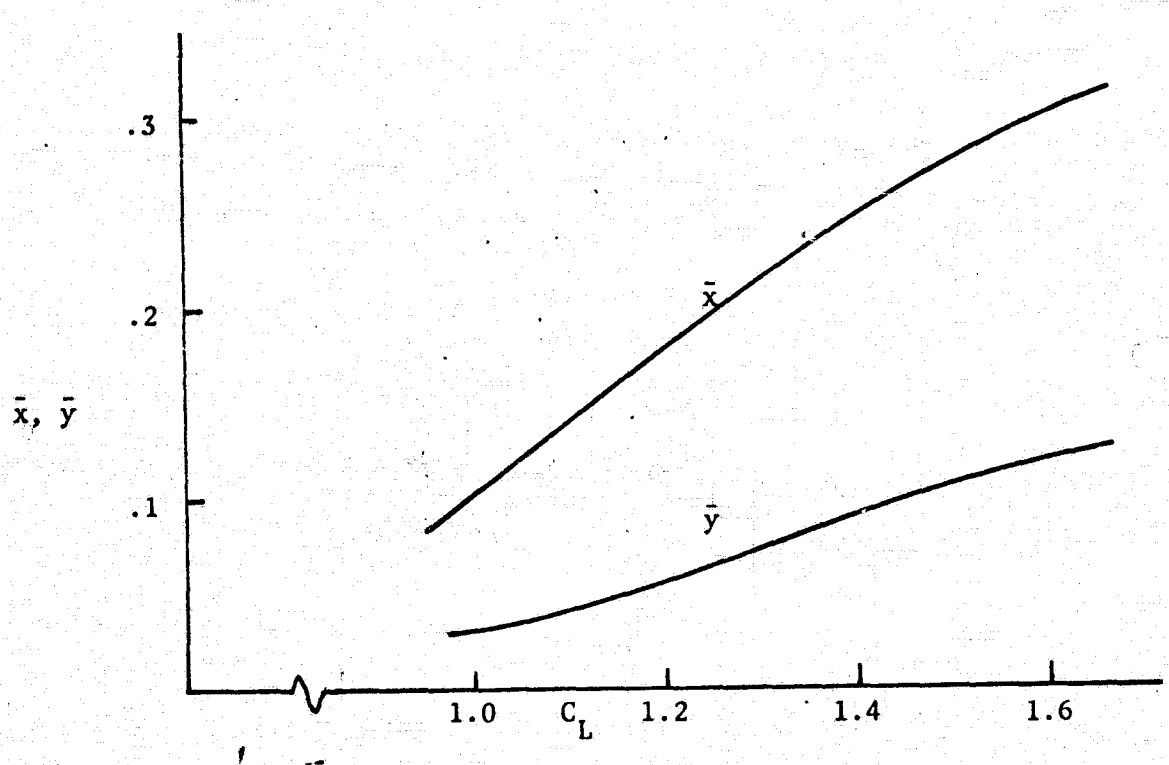

FIGURE 9. ADDITIONAL THICKNESS DISTRIBUTION TO MINIMIZE PEAK PRESSURE

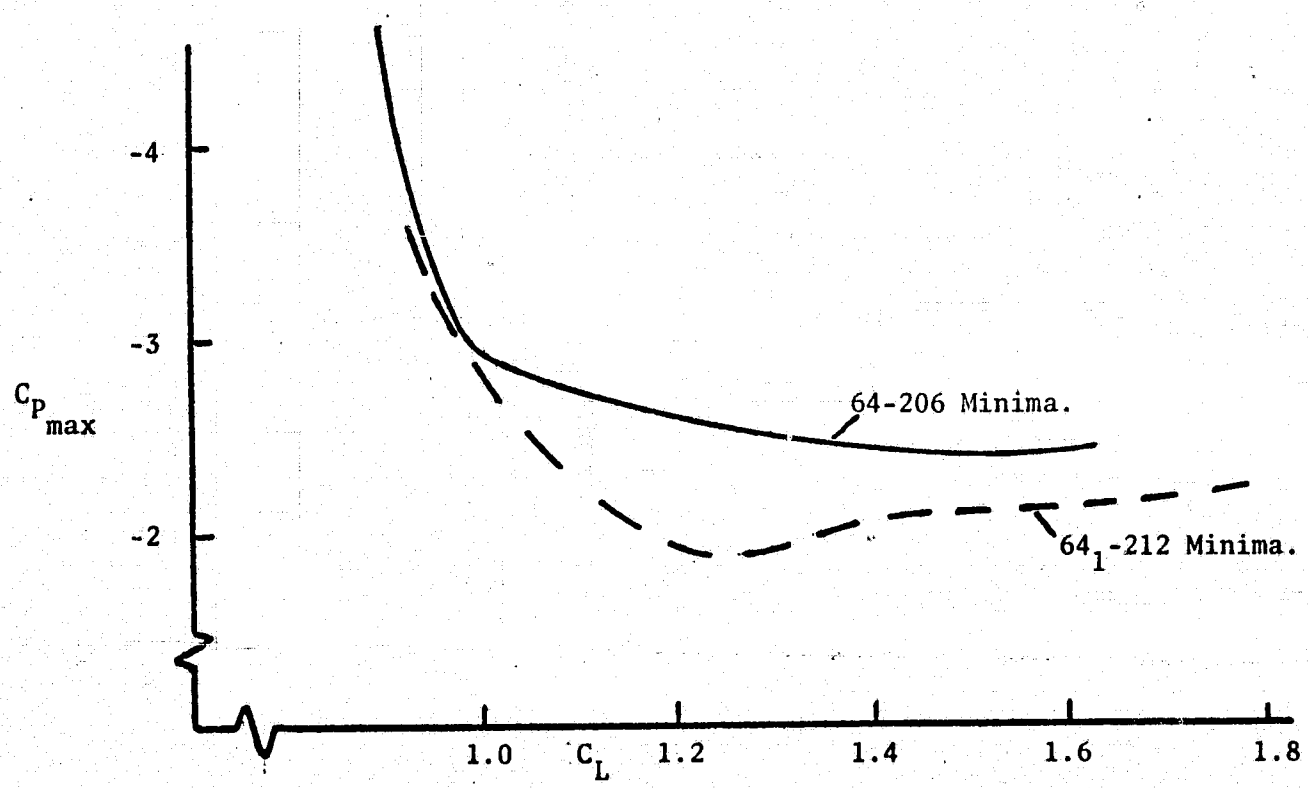

FIGURE 10. MINIMUM PEAK PRESSURE OBTAINABLE WITH BIQUADRATIC MODIFICATIONS

REFERENCES

1. Hicks, R. M., Merman, E. M., and Vanderplaatz, G. N., "Assessment of Airfoil Design by Numerical Optimization," NASA TMX-3092, July 1974.

2. Liebeck, R. H., "A Class of Airfoils Designed for High Lift in Incompressible Flow," J. Aircraft, Vol. 10, No. 10, October 1973.

3. Hague, D. S. and Glatt, C. R., "An Introduction to Multivariable Search Techniques for Parameter Optimization (and Program AESOP)," NASA CR73200, April 1968.

4. Hague, D. S., and Merz, A. W., "An Investigation on the Effect of Second-Order Additional Thickness Distributions to the Upper Surface of an NACA 64_1-212 Airfoil," Aerophysics Research Corporation TN-194, January 1975.

5. Jameson, A. "Transonic Flow Calculations for Airfoils and Bodies of Revolution," Grumman Aerodynamics Report 390-71, December 1971.

TABLE I

CONVERGENCE FOR C_L MAXIMIZATION

			$\bar{x}$	$\bar{y}$	$-C_L$
M	C	JJJ	ALPHA(1)	ALPHA(2)	FUNCTN(1)
0	1	1	.2500	1.0000E-03	-.8941
10	1	2	.2508	1.0365E-03	-.8942
10	1	3	.2583	1.1667E-03	-.8952
10	1	5	.2626	1.4155E-03	-.8968
2	1	6	.2753	1.8311E-03	-.8982
2	1	7	.2879	2.2466E-03	-.9022
2	1	8	.3132	3.0776E-03	-.9078
2	1	9	.3638	4.7398E-03	-.9196
10	2	10	.3688	4.7533E-03	-.9198
10	2	11	.3758	5.2172E-03	-.9216
10	2	12	.3824	5.5611E-03	-.9258
2	2	13	.4010	6.3824E-03	-.9320
2	2	14	.4196	7.2037E-03	-.9385
2	2	15	.4567	8.8462E-03	-.9520
2	2	16	.5311	1.2131E-02	-.9826
10	3	17	.5505	1.2761E-02	-.9863
10	3	18	.5675	1.2812E-02	-.9920
10	3	20	.5808	1.3494E-02	-.9993
2	3	21	.6305	1.4856E-02	-1.018
2	3	22	.6802	1.6219E-02	-1.041
2	3	23	.7796	1.8944E-02	-1.105
2	3	24	.9000	2.4394E-02	-1.303
10	4	25	.9000	2.5016E-02	-1.313
10	4	26	.9000	2.7157E-02	-1.350
10	4	27	.9000	3.0116E-02	-1.399
2	4	28	.9000	3.5838E-02	-1.493
2	4	29	.9000	4.1560E-02	-1.586
2	4	30	.9000	5.3003E-02	-1.765